DEFORMATION LIMIT STATES FOR CIRCULAR REINFORCED CONCRETE BRIDGE COLUMNS

By Mervyn J. Kowalsky,[1] Associate Member, ASCE

ABSTRACT: Through the use of moment-curvature analysis of circular bridge columns, dimensionless serviceability and damage control curvature relationships are developed that depend only on the column axial load ratio and section diameter. These relationships are used to establish curvature, displacement ductility, drift ratio, and equivalent viscous damping capacities for the design limit states considered. It is shown that current code-based design approaches, which imply a constant ductility factor, will generally result in damage levels that are highly variable. The paper also discusses implications of the study on limit-states design approaches such as displacement-based design.

INTRODUCTION

Many current efforts in the development of seismic design procedures fall in the category of ''performance-based'' or ''limit-states'' design. Regardless of the nomenclature, the main objective is to specify the structural performance for a given earthquake within the accuracy of current analytical techniques. In general, the structural performance is specified at not only the traditional life-safety level but also more restrictive limit states such as serviceability and damage control.

In order to control structural performance for discrete earthquake levels, it is important to consider the state of the structure at the design limit state. In the case of the damage control and survival limit states, and to a lesser extent the serviceability limit state, this requires consideration of inelastic action. As a result, deformation quantities such as strain, curvature, and displacement become paramount in the seismic design process.

Recent research (Priestley et al. 1996) has resulted in the recognition that the current basis of the force-based seismic design approach is based largely on inaccurate assumptions. In the force-based design approach, stiffness is assumed to be the fundamental section property, and as a result, forces are distributed between members in proportion to their elastic stiffness. However, a series of moment-curvature analysis on reinforced concrete bridge columns has identified section yield curvature as the more fundamental property (Priestley et al 1996).

A recent paper by Priestley and Kowalsky (1998) had as one of its objectives the development of dimensionless yield, serviceability, and damage control curvatures for structural wall buildings. It was shown that all three curvature limit states, which were defined by concrete and steel strain limits, were largely independent of axial load, longitudinal reinforcement, and distribution of longitudinal reinforcement. As in the case for circular bridge columns, section yield curvature and hence yield displacement are calculated without reference to member strength and are dependent only on the reinforcement yield strain and section depth.

In the case of circular reinforced concrete bridge columns, if it can be shown that curvatures at strain limit states other than yield can be identified with reference to variables that are typically established at the outset of the design process, then application of design procedures such as displacement-based design could be more readily achieved. Furthermore, it is expected that investigation of typical design variables such as curvature, drift, ductility, and equivalent viscous damping at limit states defined by constant strain will illustrate that uniform damage cannot in general be achieved with uniform force-reduction or ductility factors that are typical in current design methods.

In this paper, the feasibility of dimensionless curvature limit states for circular reinforced concrete bridge columns is explored. This is then followed by an investigation of trends of key design parameters and their influence on force-based and displacement-based design approaches.

DEFINITION OF LIMIT STATES

Before proceeding with the development of the dimensionless curvature relationships, the limit states adopted in this paper must be defined. Two limit states are considered in this paper: ''serviceability'' and ''damage control.'' Qualitatively, ''serviceability'' implies that repair is not needed after the earthquake, while ''damage control'' implies that only repairable damage occurs. Quantitatively, it is assumed that these limit states can be characterized with respect to concrete compression and steel tension strain limits. These limits are listed in Table 1.

The serviceability concrete compression strain is defined as the strain at which crushing is expected to begin, while the serviceability steel tension strain is defined as the strain at which residual crack widths would exceed 1 mm, thus likely requiring repair (Priestley et al. 1996) and interrupting serviceability.

The damage control concrete compression strain is defined as the compression strain at which the concrete is still repairable. This assessment is subjective and is a function of the transverse reinforcement details provided. The energy balance approach developed by Mander et al. (1988) can be utilized to estimate the ''ultimate concrete compression strain.'' This choice is based on the observation that experimental test results have shown that the ultimate concrete compression strain from this approach is consistently conservative by 50% or more when a spiral fracture strain capacity of 12% is assumed in the calculation (Priestley et al. 1996). Given the consistent level of conservatism of the energy balance approach, it is felt to be reasonable to base damage control concrete compression strain levels on the approach, recognizing that failure would

TABLE 1. Limit State Definitions

Limit state (1)	Concrete strain limit (2)	Steel strain limit (3)
Serviceability	0.004 (compression)	0.015 (tension)
Damage control	0.018 (compression)	0.060 (tension)

[1]Asst. Prof., Dept. of Civ. Engrg., North Carolina State Univ., Raleigh, NC. E-mail: kowalsky@eos.ncsu.edu

Note. Associate Editor: Takeru Igusa. Discussion open until January 1, 2001. To extend the closing date one month, a written request must be filed with the ASCE Manager of Journals. The manuscript for this paper was submitted for review and possible publication on December 9, 1998. This paper is part of the ***Journal of Structural Engineering***, Vol. 126, No. 8, August, 2000. ©ASCE, ISSN 0733-9445/00/0008-0869–0878/$8.00 + $.50 per page. Paper No. 19851.

not occur until strain levels increase by at least 50% over the damage control strain.

The damage control concrete strain of 0.018 was obtained by considering typical levels of bridge column transverse reinforcement (0.8% to 1%), spiral yield stress (450 MPa), and allowable spiral strain (0.10). Reinforced concrete columns with reinforcement details in this range have exhibited damage that would be easily repairable, and, in one case, shake table tests were performed that illustrated the repairability of a bridge subjected to this level of compression strain (Kowalsky et al. 1997).

The remaining limit state definition is related to the steel tension strain at the damage control level. The point at which repair no longer becomes feasible will likely be related to the point at which incipient buckling of reinforcement occurs, which may in turn be related to the peak tension strain sustained in the previous loading cycle. At this time, insufficient data exist to quantify this limit. However, the steel tension strain must also be limited to avoid rupture of reinforcement while allowing for the reduction in strain capacity due to cyclic loading. The limit shown in Table 1 is based on this condition (Priestley et al. 1996).

The damage control level strain limits discussed here are not sacred, and other definitions can be established. However, the limits are felt to be consistent with experimental observations and transverse reinforcement details that are typically employed for reinforced concrete bridge columns. It is also noted that the damage control level strain limits assume well-detailed systems, and would not be appropriate for assessment of existing columns with insufficient transverse reinforcement. In the case of the serviceability limit state, the proposed strain limits are felt to be widely accepted.

DIMENSIONLESS CURVATURE RELATIONS AT DESIGN LIMIT STATES

Previous research (Priestley et al. 1996) has resulted in the development of a simple relationship for the yield curvature of a circular reinforced concrete column section. The equation is shown as (1) and is a function only of the section diameter and longitudinal bar yield strain, ε_Y. A moment-curvature analysis is shown in Fig. 1 where each of the limit states is shown by an arrow. The yield curvature, ϕ_y, is calculated by extrapolating the first yield curvature, ϕ'_y, to the nominal flexural strength, M_n, as shown in Fig. 1.

$$\phi_Y D = 2.45\varepsilon_Y = K_Y \pm 15\% \tag{1}$$

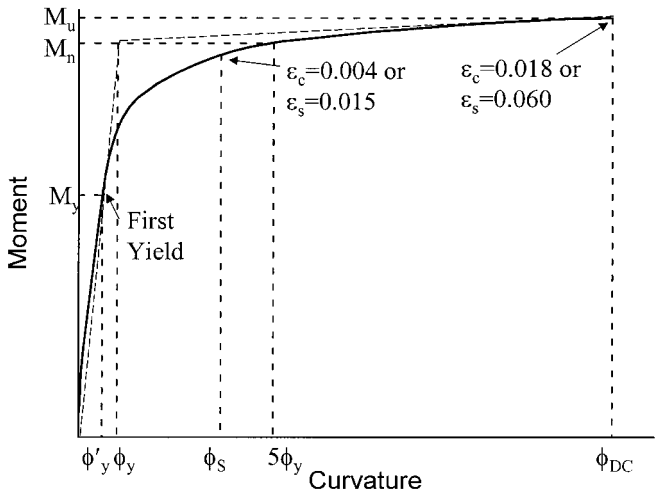

FIG. 1. Definition of Limit States from Moment-Curvature Analysis

In the research described in this paper, a series of moment-curvature analyses was performed on circular columns with varying levels of axial load ratio and longitudinal reinforcement ratio. The axial load was varied from 0 to $0.4f'_cA_g$ while reinforcement ratios were varied from 1 to 4% of the gross section area. The objective of the analysis was to identify any trends in serviceability and damage control curvatures for circular columns. The analyses were carried out with a computer program (King et al. 1986) that performs moment-curvature analysis. Since future research will likely provide refined strain limits, particularly at the damage control level, section curvatures were tabulated for concrete compression strains of ε_c = 0.004, 0.010, 0.018, 0.030, 0.040 and steel tension strains of ε_s = 0.015, 0.030, 0.040, 0.060, 0,090 across the range of variables considered. The baseline section consisted of a circular columns section 1 m in diameter. The concrete compressive strength was 28 MPa, while the yield stress of all reinforcement was 450 MPa. The longitudinal bar diameter was chosen as 35 mm, and the transverse volumetric steel ratio was 1%. The concrete cover to the main reinforcement was 50 mm. Results of the analyses are normalized according to section diameter and are plotted versus axial load ratio for the four longitudinal steel ratios considered. Results are shown in Fig. 2. In each case, the solid lines represent limit state curvatures based on concrete compression strains and the dashed lines represent the limit state curvatures based on constant steel tension strains.

From the analysis results, it is clear that the section curvatures at constant concrete compression strains are strongly influenced by longitudinal steel ratio, particularly when combined with low axial load levels. It is also noted that section curvatures at constant steel tension strains show very little variation with longitudinal steel ratio.

Utilizing the strain limits suggested in Table 1 and referring to Fig. 2, the dimensionless curvatures for the serviceability and damage control limit states can be extracted as shown in Figs. 3 and 4. Linear fits to the data are also shown in Figs. 3 and 4 along with ±15% deviation lines, shown as dashed.

For the serviceability limit state (Fig. 3), the proposed expression [(2)] yields good results across the range with the exception of the case where low axial load is combined with low steel percentage. Clearly, better results could be obtained by considering a polynomial expression that is also a function of steel ratio; however, for the majority of the cases, the added complexity would not be warranted. Furthermore, the objective here is to obtain a reasonable estimate of limit-state curvatures with the information typically available at the onset of the design process, that is, column diameter and axial load ratio. For cases where reinforcement is low and is known at the outset, Fig. 2 could be used directly to make a more refined estimate of serviceability limit state curvature.

Fig. 4 presents the results for the damage control limit state, and (3) represents the linear fit to the data. Note that the agreement is somewhat better for the damage control limit state. It is noted that the damage control curvature for the column containing an axial load ratio of 0 and a steel ratio of 1% was governed by the steel tension strain limit, whereas all others were governed by the concrete compression strain limit. As the axial load ratio and steel ratio decrease, the demand on the steel increases, and as a result the tension steel limit governs as expected.

$$\phi_S D = 0.015 - 0.020\left(\frac{P}{f'_cA_g}\right) = K_S \pm 15\% \tag{2}$$

$$\phi_{DC} D = 0.068 - 0.068\left(\frac{P}{f'_cA_g}\right) = K_{DC} \pm 15\% \tag{3}$$

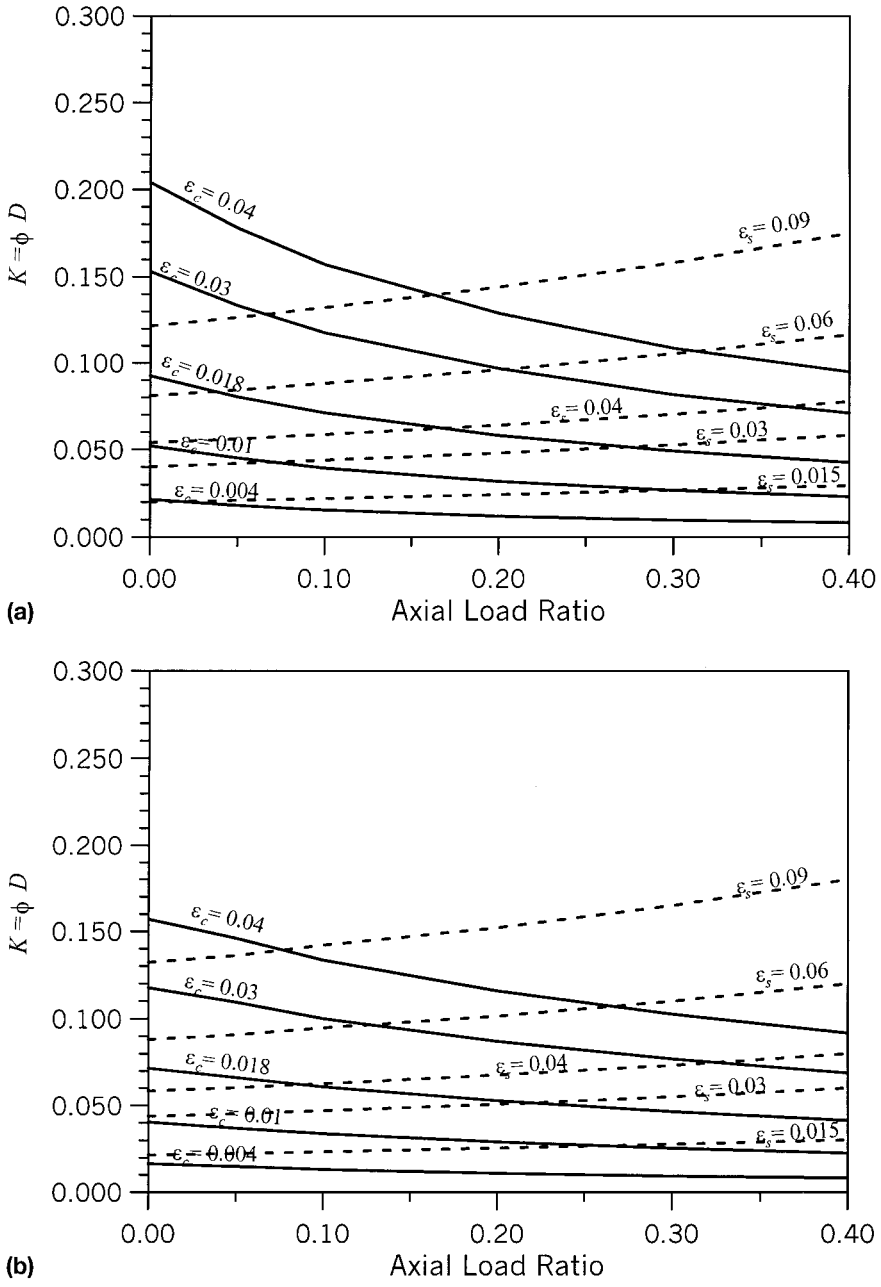

FIG. 2. Dimensionless Curvature for Lines of Equal Strain: (a) 1% Longitudinal Steel Ratio; (b) 2% Longitudinal Steel Ratio; (c) 3% Longitudinal Steel Ratio; (d) 4% Longitudinal Steel Ratio

When using (2) and (3), it is noted that *the expressions developed should not be extrapolated beyond the limits of axial load ratio and longitudinal steel ratio considered in their development*; however, most bridge columns will fit within the limits considered. Also, the combination of 1% steel ratio and an axial load ratio of 0 will underestimate the serviceability level curvature by approximately 30%. For these cases, the graphs could be used directly for a more accurate estimate of limit state curvature. The damage control limit state curvature will not apply for assessment of existing columns with insufficient transverse reinforcement, as previously mentioned.

It is also noted that as refined estimates for strain limits are developed, Fig. 2 can be utilized to obtain revised expressions for dimensionless curvatures. This is particularly important for the damage control limit state where revised tension strain limits are likely to be obtained. Fig. 2 also can be utilized for calculation of curvature at specific strain levels not considered by the limit states discussed in this paper.

DRIFT RATIOS FOR DESIGN LIMIT STATES

Having established the dimensionless curvature relationships for the two limit states discussed in this paper, closed-form expressions for the average drift ratio, $\theta = \Delta/L$, are obtained easily. The average drift ratio, θ, can be expressed for the serviceability and damage control limit states as (4) and (5), respectively:

$$\theta_S = \frac{K_S - K_Y}{D} L_p + \frac{K_Y}{3} \frac{L}{D} \tag{4}$$

$$\theta_{DC} = \frac{K_{DC} - K_Y}{D} L_p + \frac{K_Y}{3} \frac{L}{D} \tag{5}$$

In (4) and (5), L_p represents the member plastic hinge length (Priestley et al. 1996), which is given as the greater of (6*a*) and (6*b*) where d_{bl} is the longitudinal bar diameter.

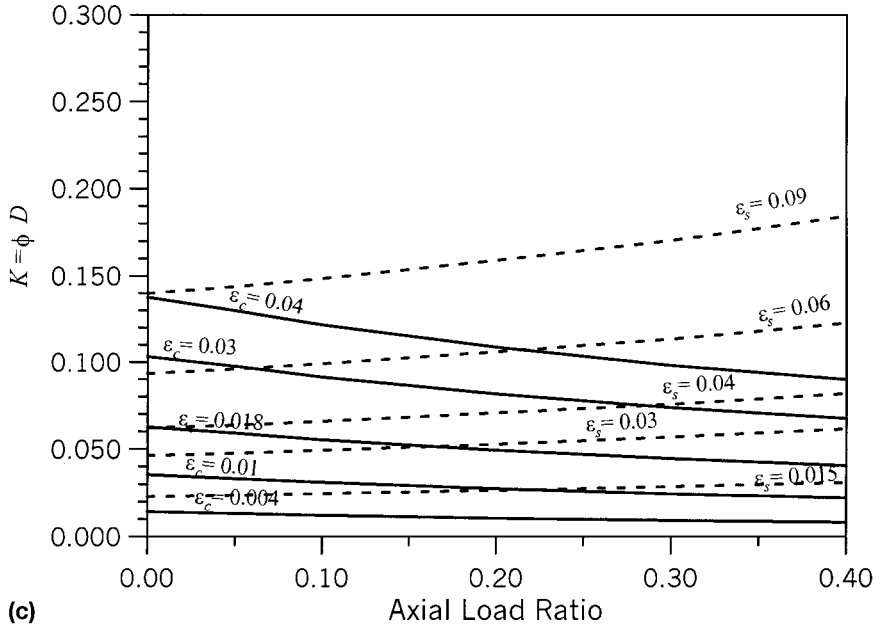

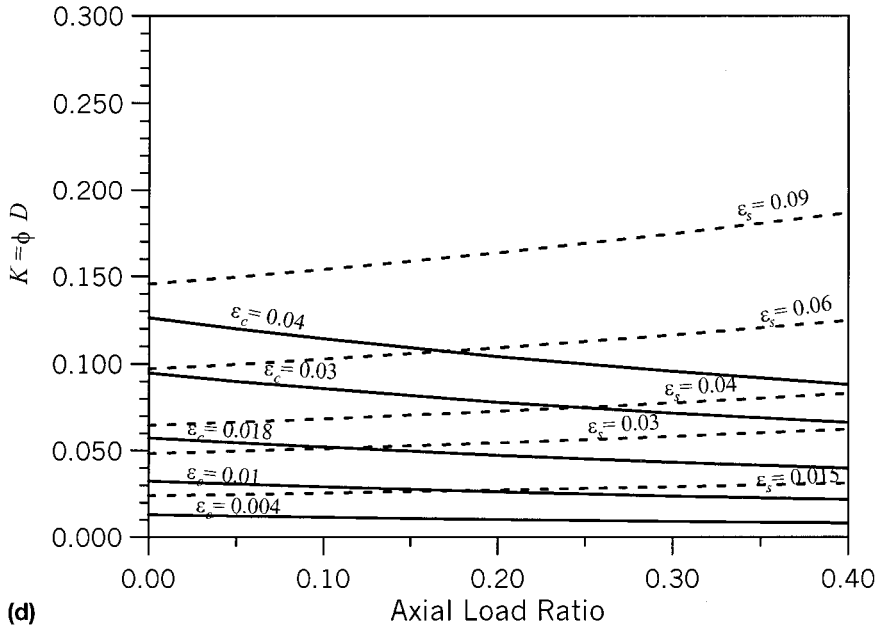

FIG. 2. (*Continued*)

$$L_p = 0.08L + 0.022 f_y d_{bl} \quad (6a)$$

$$L_p = 0.044 f_y d_{bl} \quad (6b)$$

Since (4) and (5) represent the average drift ratio for a circular reinforced concrete bridge column, the column top displacement can be obtained by multiplying θ by the column height L. In order to obtain the column displaced shape at any point, the variation in elastic rotation along the column must be calculated. However, for bridge design, typically the displacement at the bridge deck is the important design variable.

DUCTILITY AND DRIFT RATIO DEMAND TRENDS AT DESIGN LIMIT STATES

By dividing the design limit state curvatures [(2) and (3)] by the yield curvature (1), the curvature ductility factors for the serviceability, $\mu_{\phi S}$, and damage control, $\mu_{\phi DC}$, limit states are obtained. Performing that calculation results in (7) and (8), respectively. Note that a longitudinal bar yield stress of 450 MPa has been used to calculate the bar yield strain in (1).

$$\mu_{\phi S} = 3.63 \left(0.75 - \frac{P}{f'_c A_g}\right) \quad (7)$$

$$\mu_{\phi DC} = 12.34 \left(1 - \frac{P}{f'_c A_g}\right) \quad (8)$$

Curvature ductility can then be related to displacement ductility through (9) (Priestley et al. 1996):

$$\mu_\Delta = 1 + 3(\mu_\phi - 1)\frac{L_p}{L} \quad (9)$$

By introducing the variable of the aspect ratio, L/D, into the plastic hinge length expressions, (6) can be arranged into (10*a*) and (10*b*). These can then be evaluated at discrete column diameters and dimensionless expressions developed.

$$\frac{L_p}{L} = 0.08 + \frac{0.022 f_y d_{bl}}{D\left(\frac{L}{D}\right)} \quad (10a)$$

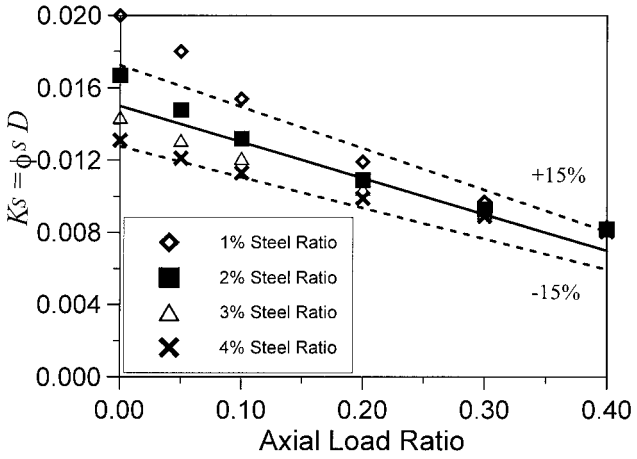

FIG. 3. Dimensionless Serviceability Curvature versus Axial Load Ratio

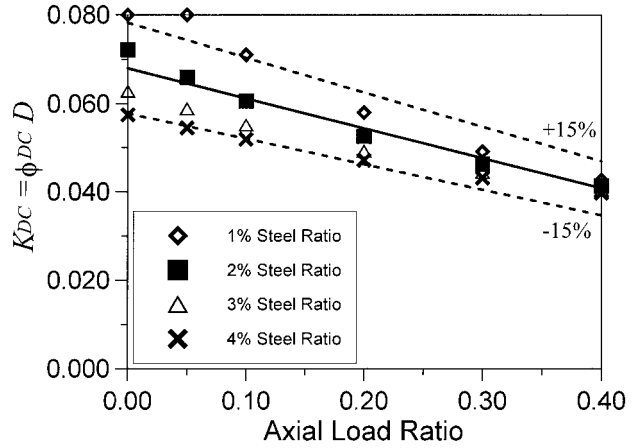

FIG. 4. Dimensionless Damage Control Curvature versus Axial Load Ratio

$$\frac{L_p}{L} = \frac{0.044 f_y d_{bl}}{D\left(\frac{L}{D}\right)} \qquad (10b)$$

Since the dimensionless plastic hinge length expressions will vary depending on the column diameter chosen, (10) was evaluated with column diameters ranging from 0.5 to 5 m, which will amply cover the likely section sizes. The results are shown in Fig. 5 where L_p/L is plotted versus the aspect ratio L/D for the various column diameters chosen. In Fig. 5, a bar diameter of 35 mm is assumed, as previously mentioned. Bridge longitudinal reinforcement would rarely be smaller, and is only occasionally much larger. Each curve represents the greater of (10) for varying column diameters. Note that as the column diameter increases, the variation of the ratio L_p/L versus the aspect ratio decreases and becomes almost constant, particularly when the diameter exceeds 1.5 m. The first term of (6*a*) was originally established such that the deformation obtained by multiplying the plastic curvature by the length L_p added to the elastic deformation would equal the deformation obtained by integration of the curvature distribution along the column height. The second term of (6*a*) was established recognizing that the curvature does not instantaneously reduce to zero due to strain penetration into the adjacent member. Eq. (6*b*) represents a minimum plastic hinge length recognizing that strain penetration occurs equally into the column and adjacent member (Priestley et al. 1996). For shorter columns (6*b*) will govern, as the length-dependent component of (6*a*) becomes small compared with the strain penetration component.

For the calculations that follow, column diameters of 0.75 m and 3 m will be utilized. Few column diameters will be smaller than 0.75 m, and the variation in plastic hinge length beyond 3 m is minimal.

Combining the greater of (10) with (7), (8), and (9) results in estimates of displacement ductility demand for both serviceability and damage control limit states. The results are shown in Fig. 6 for the serviceability limit state. Considering

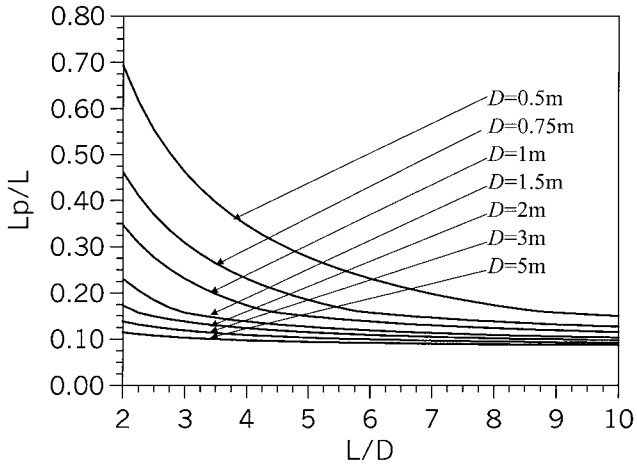

FIG. 5. Dimensionless Plastic Hinge Length versus Aspect Ratio

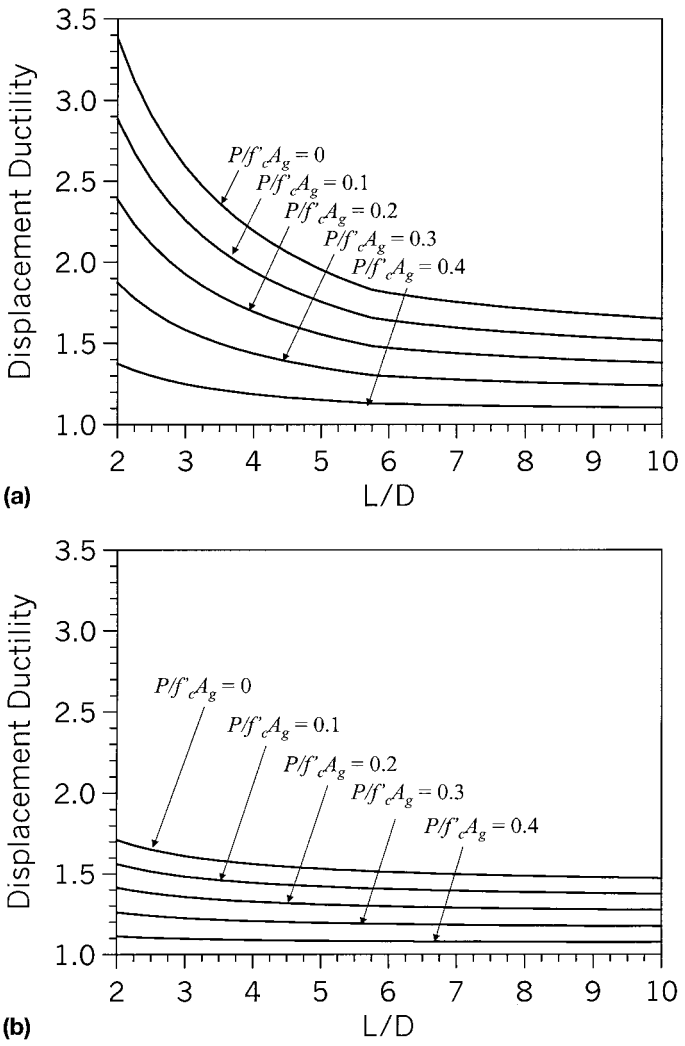

FIG. 6. Serviceability Displacement Ductility versus Aspect Ratio: (a) *D* = 0.75 m; (b) *D* = 3 m

Fig. 6(a) first (D = 0.75 m), note that the ductility demand varies between 1.4 and 3.4 for an aspect ratio of 2 and between 1.1 and 1.8 for larger aspect ratios depending on the axial load ratio. For the 3 m column diameter shown in Fig. 6(b), the variation with aspect ratio is much less pronounced. The serviceability ductility demand varies from 1.1 to 1.7 depending primarily on the axial load ratio.

For the damage control limit state, the results are shown in Fig. 7. Note that the variation in ductility demand for the 0.75 m diameter columns in Fig. 7(a) is from 10 to 17 for low aspect ratios, and from 3.6 to 5.5 for larger aspect ratios. For the 3 m diameter columns, the variation in Fig. 7(b) is from 3.7 to 5.7 at low aspect ratios, and from 2.8 to 4.3 for larger aspect ratios.

The comparison can also be made in terms of drift ratios versus column aspect ratio. Considering the serviceability limit state, the drift ratio demand is shown in Fig. 8(a) for 0.75 m diameter columns. Note that the drift ratio varies extensively with both axial load ratio and aspect ratio, from a low of 0.005 to a high of 0.03. For the 3 m diameter columns (Fig. 8b), the variation with axial load ratio is less. However, the variation with aspect ratio is extensive. In this case, drift ratios for the serviceability limit state varied from 0.004 to 0.027.

For the damage control limit state, the results are shown for the 0.75 m diameter column in Fig. 9(a). Here the variation is also extensive, ranging from 0.036 to 0.096. Similarly, for the 3 m diameter column, the variation is from 0.013 to 0.075, as shown in Fig. 9(b).

The plastic hinge length expression used in the above calculations assumes a bar diameter of 35 mm. If a bar diameter of 57 mm is employed, the change in drift ratio demand varies from 5 to 20% (damage control limit state), depending on the aspect ratio, when compared with the results assuming a 35 mm bar diameter. For the serviceability limit state, the variation is less than 5% across all aspect ratios.

Application of limit-states design approaches such as displacement-based design (Priestley 1993; Calvi and Kingsley 1995; Kowalsky et al. 1995) utilize the concept of equivalent viscous damping (Jacobsen 1930; Gulkan and Sozen 1974; Shibata and Sozen 1976) for characterizing the inelastic behavior of the system. The equivalent viscous damping concept rigorously replaces the force reduction or ''behavior modification factor'' inherent in current force-based design methods. As a result, investigation of trends related to equivalent viscous damping at the design limit states is worthwhile.

Relations between equivalent viscous damping and displacement ductility can be established for an assumed hysteretic response. For well-detailed reinforced concrete columns, the response can be characterized with the Takeda degrading stiffness hysteretic response (Takeda et al. 1970). Eq. (11) represents the damping-ductility relationship for the Takeda degrading stiffness hysteretic response (Kowalsky et al. 1995), where r represents the second slope stiffness ratio (0.05 in this paper). Also assumed in (11) is a viscous damping ratio of 0.05 that is additive to the equivalent viscous damping obtained from the hysteretic energy dissipation.

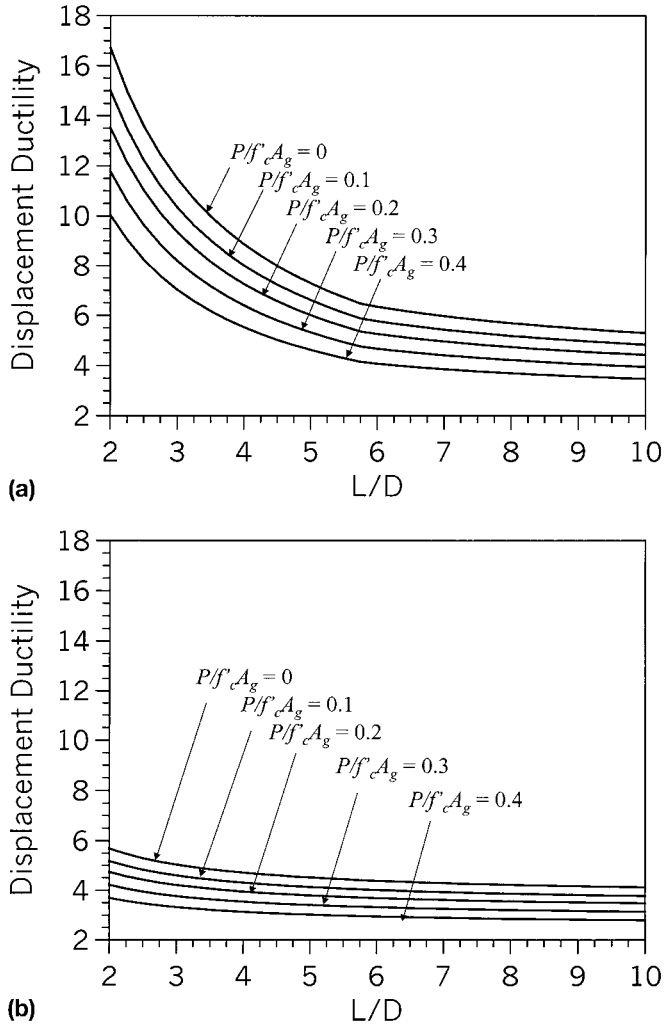

FIG. 7. Damage Control Displacement Ductility versus Aspect Ratio: (a) D = 0.75 m; (b) D = 3 m

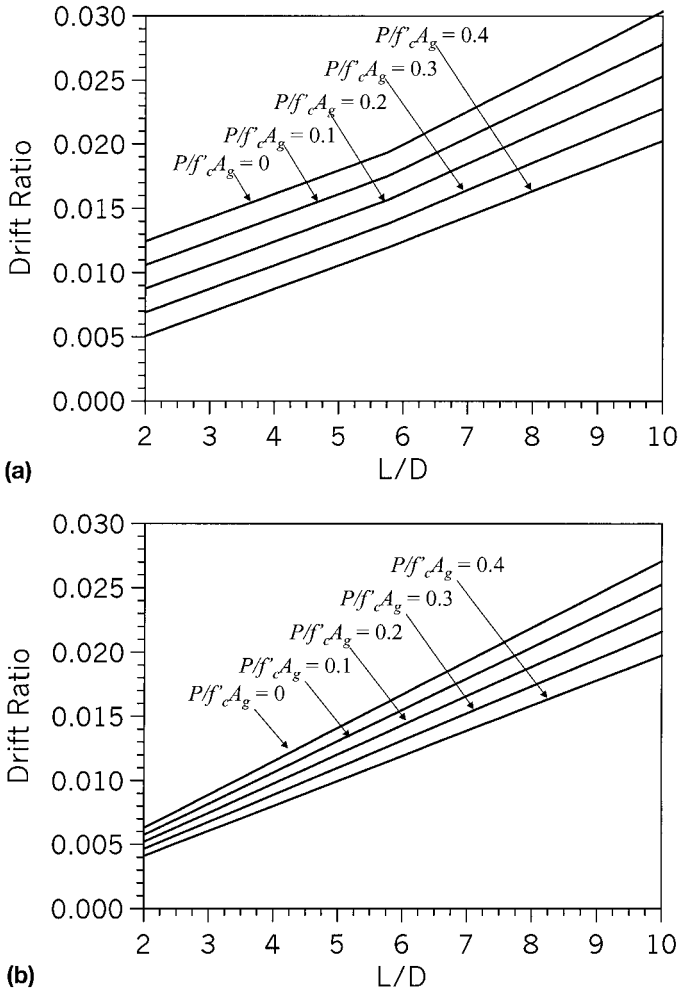

FIG. 8. Serviceability Drift Ratio versus Aspect Ratio: (a) D = 0.75 m; (b) D = 3 m

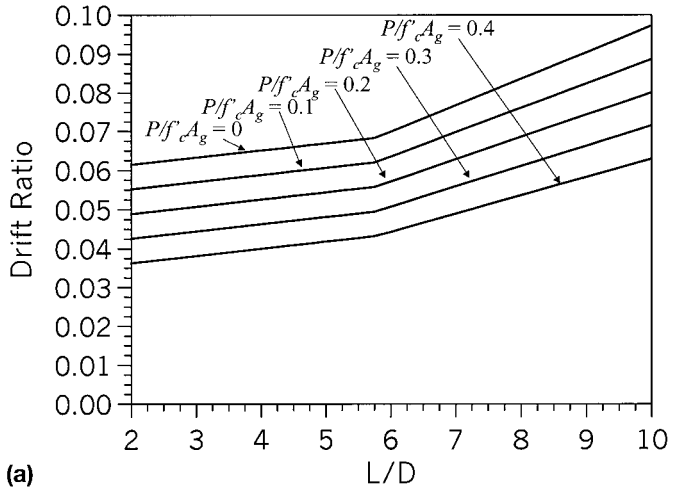

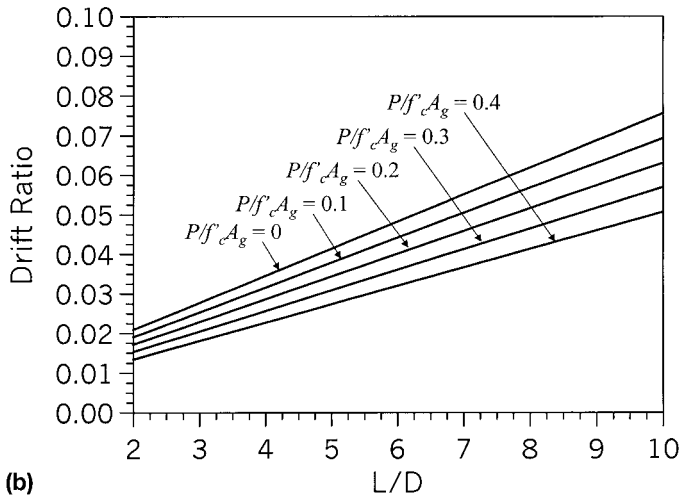

FIG. 9. Damage Control Drift Ratio versus Aspect Ratio: (a) D = 0.75 m; (b) D = 3 m

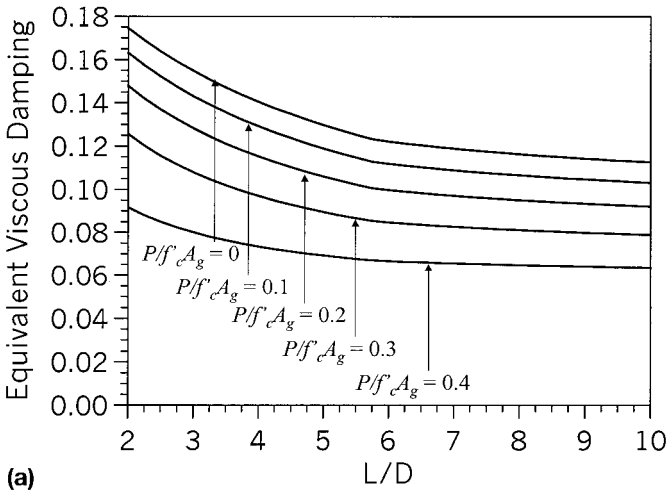

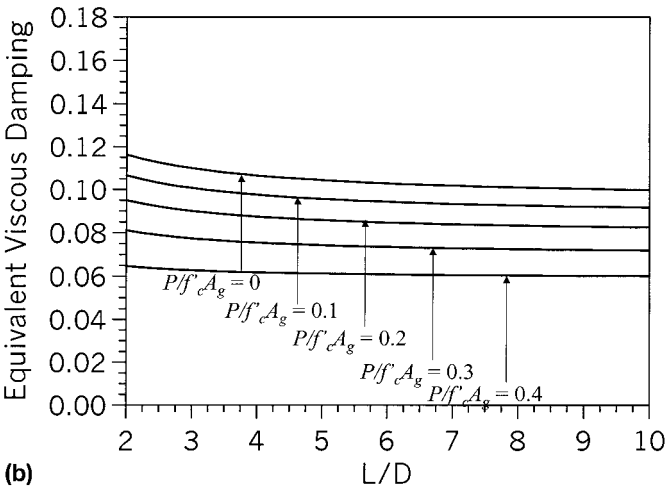

FIG. 10. Serviceability Equivalent Viscous Damping versus Aspect Ratio: (a) D = 0.75 m; (b) D = 3 m

$$\zeta = 0.05 + \frac{1 - \frac{1 - r}{\sqrt{\mu_\Delta}} - r\sqrt{\mu_\Delta}}{\pi} \tag{11}$$

Using the data in Figs. 6 and 7 and (11), equivalent viscous damping trends can be investigated. Fig. 10(a) represents the serviceability limit-state equivalent viscous damping for columns with a diameter of D = 0.75 m. As expected, and following the variation in displacement ductility, equivalent viscous damping remains essentially constant for a given axial load ratio beyond an aspect ratio of 6. For the 3 m column [Fig. 10(b)], the damping is almost constant across the range of aspect ratios and varies only with axial load ratio. For the damage control limit state (Fig. 11), the variation is less pronounced. Although it may appear that constant damping values may be employed for a column of given axial load ratio, it appears that generalizations across all columns may be overly coarse.

IMPLICATIONS FOR CURRENT BRIDGE DESIGN PRACTICE

Upon examination of the trends shown in Figs. 6–9, it is apparent that the ductility and drift demand to achieve the same damage level will vary highly with the geometry of the column. That is, if uniform serviceability in a moderate earthquake or uniform repairable damage in a large earthquake across all columns is desired, the ductility and drift demands will vary depending on the column aspect ratios.

As an example, consider the ATC-32 (Applied Technology Council 1996) bridge design recommendations. The ATC-32 document is intended to provide guidelines for a ''functional'' evaluation (serviceability), and a ''safety'' evaluation (damage control or survival limit states). The criteria for serviceability described in ATC-32 are a concrete compression strain limit of 0.004 and a steel tension strain limit of 0.010, (which is less than the 0.015 adopted here). For the functional evaluation in the ATC-32 guidelines, elastic response is assumed and a ductility level of one is implied. Comparing this with the ductility demands shown in Fig. 6 illustrates an inconsistency within the ATC-32 force-based approach. That is, the ATC-32 strain limits and the implied ductility of 1 will rarely coincide. In most cases, the ductility demand to reach the serviceability limit state will be greater than 1, particularly for the smaller diameter columns. As a result, a serviceability level design with a force reduction factor of 1 would be expected to yield a conservative result. Furthermore, from this comparison it is apparent that strain and ductility targets cannot both be specified and attempts to satisfy both criteria will in many cases not be achievable.

For the damage control level, the ATC-32 document implies a ductility demand of 4 that is constant for all ''full ductility, well confined'' systems. Referring to Fig. 7(a), it is clear that in order for ductility to remain constant at 4 for columns of different geometry, damage would vary greatly depending on aspect ratio. For the larger column diameter [Fig. 7(b)], the ductility demand is essentially constant, indicating that a con-

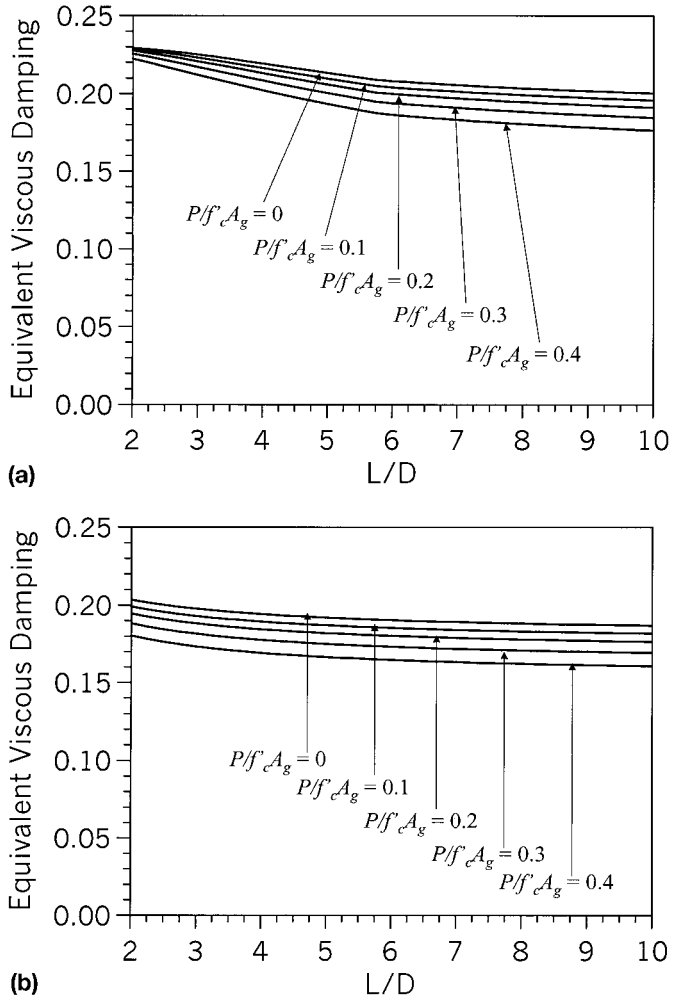

FIG. 11. Damage Control Equivalent Viscous Damping: (a) D = 0.75 m; (b) D = 3 m

stant force reduction factor of 4 should yield essentially constant damage. However, it is noted that for aspect ratios beyond approximately 6, the drift ratios required to achieve a ductility level of 4 become excessive (beyond 5%). This is a direct result of the higher elastic flexibility of columns with larger aspect ratios, which results in comparatively larger elastic deformation and hence total deformation.

As a further example illustrating the implication of using a force reduction factor that is constant for all columns in a bridge, consider a bridge configured with columns 14, 7, and 21 m tall (in that order) each supporting an axial load of $0.1f'_cA_g$ and separated by 50 m spans. Let the column diameter in each case by 3 m. The drift ratio demands for constant damage in the three columns would be approximately 3.6, 2.2, and 5%. This coincides with displacements of 500, 154, and 1,050 mm. A superstructure with even minimal rigidity would not allow such a displacement pattern to develop, with the result being a reduced displacement at the tail exterior columns and increased displacement and hence damage in the central column. Furthermore, inelastic displacements in the force-based approach are typically estimated by the equal-displacement approximation, which will tend to overestimate the deformation of columns that remain essentially elastic. A more rational approach would consider the displacement and hence ductility demands of each column individually in conjunction with superstructure rigidity in assessing the design base shear force.

IMPLICATIONS ON LIMIT-STATES DESIGN

The primary implication of the work described in this paper on limit-states design approaches such as displacement-based design is the relative ease with which target displacements can be obtained. Column target drift ratios can be directly obtained form Figs. 8 and 9 or calculated using Fig. 2 and simple expressions relating curvature to drift ratio. Equivalent viscous damping can also be obtained readily from Figs. 10 and 11. For multiple bent bridges, it must be recognized that not all columns can achieve their limit state displacement, and the overall displaced shape for a bridge must reflect this.

Since it is likely that multiple limit states will be considered in the design of a bridge, it is worthwhile to determine if criteria for identification of the critical design limit state can be readily achieved.

In order to develop this criteria, a simplified base shear equation for displacement-based design is developed that relates the target displacement, Δ_{tar}, equivalent viscous damping (expressed as a percentage), ζ_{eff}, system effective mass, m_{eff}, and response spectrum characteristics to design base shear force. In order to develop this expression, a brief summary of the direct displacement-based design approach is provided. The displacement-based design approach (Kowalsky et al. 1995) is a spectral-based design procedure that utilizes target displacement as the starting point and concludes with required strength. Traditional parameters such as initial stiffness and period are not utilized in the displacement-based design approach. In the displacement-based design procedure, the substitute structure approach (Shibata and Sozen 1976) is utilized to characterize the inelastic system with equivalent elastic properties.

Referring to Fig. 12, the displacement-based design procedure starts by entering the design displacement response spectra with the chosen target displacement, Δ_{tar}, and reading across to the appropriate response curve and down to the effective period, T_{eff} [Fig. 12(a)]. Note that the appropriate response curve is determined from the level of equivalent viscous damping that is calculated from the displacement ductility (target displacement divided by yield displacement) as shown in Fig. 12(b). For circular bridge columns, the yield curvature is obtained directly from (1). Yield curvature is then easily converted to yield displacement. If the column diameter is not known at the outset, the procedure converges onto a required yield displacement and hence column diameter, as well as required strength (Kowalsky et al. 1995).

The displacement response spectra at damping values other than 5% can be obtained utilizing relations such as that proposed by the Eurocode [(12)] (Commission of the European Communities 1988). If the displacement response spectra is linear as shown in Fig. 12(a), a closed-form expression for the effective period, T_{eff}, as a function of the target displacement, Δ_{tar}, equivalent viscous damping, ζ_{eff}, and spectral parameters Δ_c and T_c [shown in Fig. 12(a)] can be obtained as shown in (13)

$$\Delta_\zeta = \Delta_{5\%} \sqrt{\left(\frac{7}{2 + \zeta_{eff}}\right)} \tag{12}$$

$$T_{eff} = \Delta_{tar} \frac{T_c}{\Delta_c \sqrt{\dfrac{7}{2 + \zeta_{eff}}}} \tag{13}$$

Utilizing the equation for a single-degree-of-freedom oscillator, the effective stiffness of the structure is obtained and is shown as (14). The required base shear force is then obtained by multiplying the effective stiffness by the design target displacement as in Fig. 12(c). The final expression is shown as (15). Note that (15) applies equally well for multiple-degree-

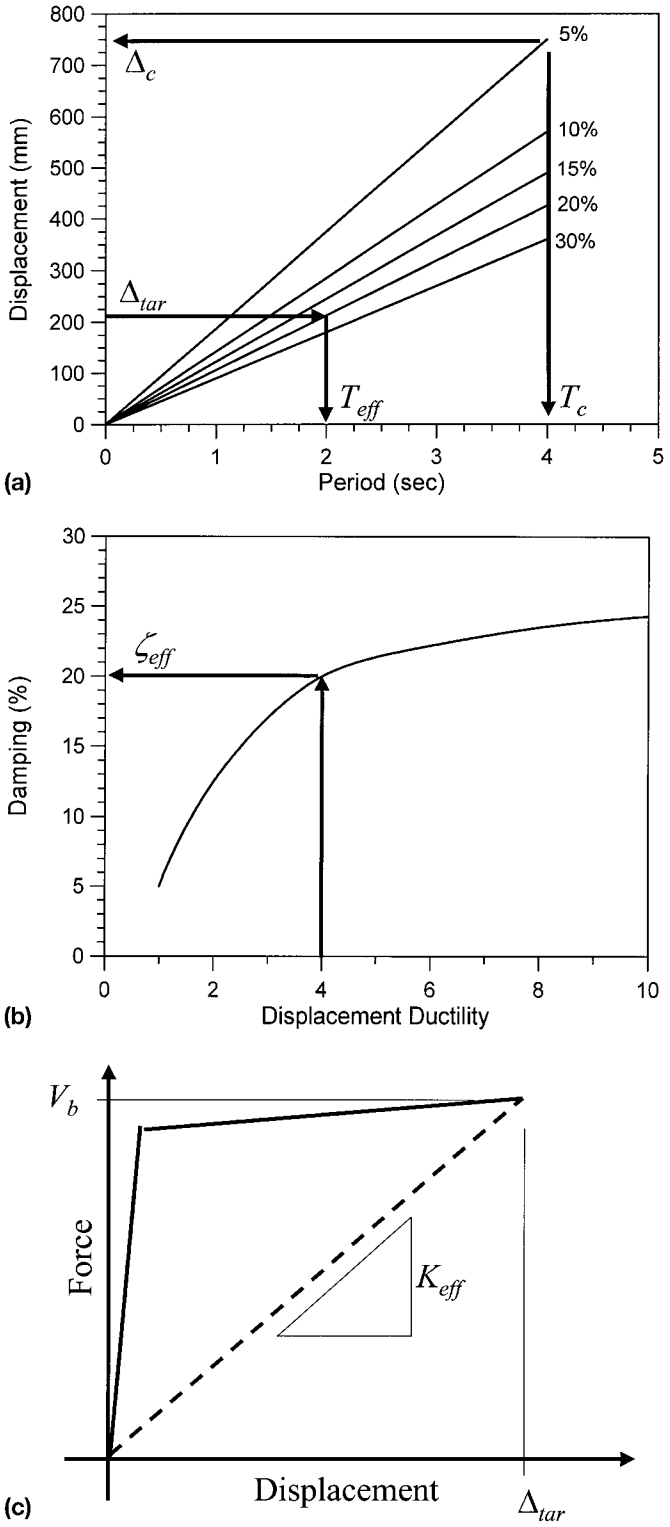

FIG. 12. Overview of Displacement-Based Design: (a) Obtaining Effective Period; (b) Obtaining Equivalent Viscous Damping; (c) Obtaining Design Base Shear Force

of-freedom systems as long as the target displacement, effective mass, and equivalent viscous damping are evaluated for an equivalent single-degree-of-freedom system. Models for such systems are obtained in the literature (Shibata and Sozen 1976; Calvi and Kingsley 1995)

$$k_{\text{eff}} = \frac{4\pi^2 m_{\text{eff}}}{T_{\text{eff}}^2} = \frac{4\pi^2 m_{\text{eff}}}{\Delta_{\text{tar}}^2} \frac{\Delta_c^2}{T_c^2} \frac{7}{2 + \zeta_{\text{eff}}} \tag{14}$$

$$V_b = \frac{4\pi^2 m_{\text{eff}}}{\Delta_{\text{tar}}} \frac{\Delta_c^2}{T_c^2} \frac{7}{2 + \zeta_{\text{eff}}} \tag{15}$$

Design of the structure then proceeds by distributing the base shear to the columns in proportion to their effective stiffness and designing longitudinal reinforcement to resist the moment demand and the transverse reinforcement to resist the strain demand for the chosen limit state.

A useful result that follows from (15) is the ability to readily identify the critical design level when performing a multilevel design. For each design limit state considered, a value for the target displacement and equivalent viscous damping [Δ_{tar} and ζ_{eff} in (15)] is obtained. Furthermore, the earthquake for which that performance is desired will be identified by its response spectrum [Δ_c and T_c in (15)]. Taken together, a design limit state and its corresponding earthquake intensity represent a performance level. The ratio of earthquake intensities (serviceability level earthquake/damage control level earthquake) that results in the same base shear force for the two limit states is then obtained by (16). Although the study here focuses on the serviceability and damage control limit states, (16) applies to any two limit states

$$\frac{\Delta_{cS}}{\Delta_{cDC}} = \sqrt{\frac{2 + \zeta_{\text{eff}S}}{2 + \zeta_{\text{eff}DC}} \frac{\Delta_{\text{tar}S}}{\Delta_{\text{tar}DC}}} \tag{16}$$

Given the target displacements for each of the two design limit states and the corresponding equivalent viscous damping, the critical earthquake intensity ratio can be established. This can then be compared to the actual ratio of the earthquake for

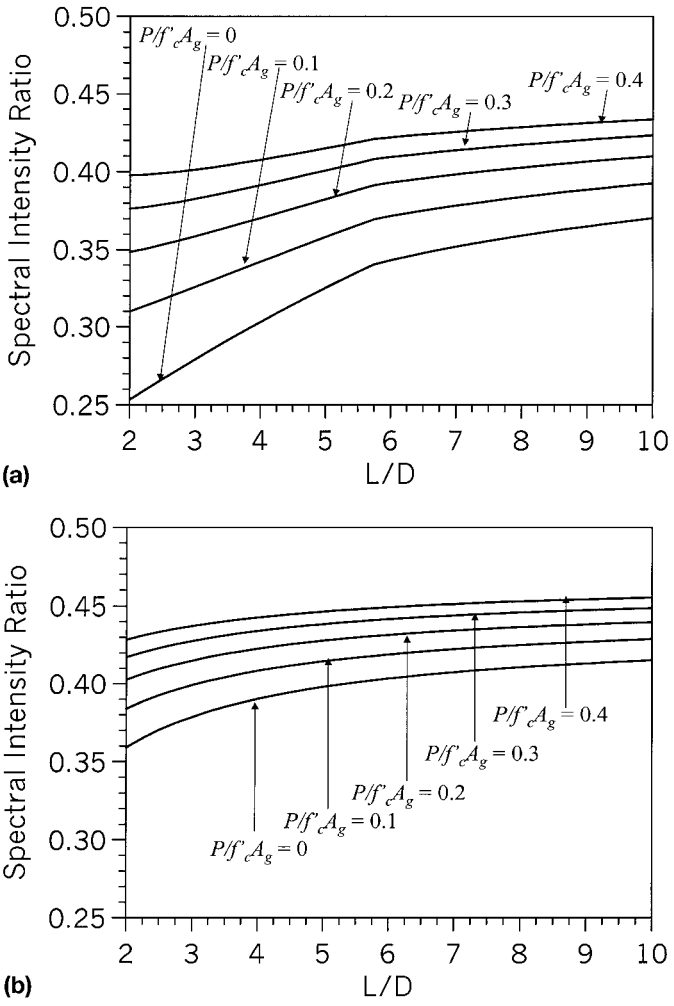

FIG. 13. Spectral Intensity Ratio: (a) *D* = 0.75 m; (b) *D* = 3 m

which serviceability level performance is desired to the earthquake for which damage control level performance is desired to determine which limit state will govern the design. If the ratio exceeds the value from (16), then the serviceability limit state will govern the design. If it is less, then the damage control limit state will govern. Using the data from Figs. 8–11 and (16), trends in the critical spectral intensity ratio can be established. The results are shown in Fig. 13.

The earthquake for which serviceability level performance is desired and the earthquake for which damage control performance is desired will largely be a matter of choice. It will be a function of the importance of the building as well as the seismicity of the region. If serviceability level performance is desired for a 50-year return period, and damage control performance for a 500 year return period, then for regions of high seismicity it can be assumed that the serviceability level event will be approximately 40% (Pauley and Priestley 1992) of the damage control level event. Returning to Fig. 13, it is then clear that for many cases the serviceability limit state may govern the design of the system.

CONCLUSIONS

The objectives of this paper were as follows: (1) Develop dimensionless serviceability and damage-control curvature relationships for circular reinforced concrete bridge columns; (2) identify trends in curvature ductility, displacement ductility, drift ratio, and equivalent viscous damping demands for the design limit states; and (3) discuss implications of the deformation trends on current force-based design approaches and more recent displacement-based approaches. From the results shown, it was concluded that simple relationships between limit state curvatures, section diameter, and axial load ratio are possible. The resulting relationships were utilized to illustrate the variations in drift, ductility, and equivalent viscous damping for columns of different aspect ratios. It was also shown that design procedures that imply the use of constant ductility may yield highly variable levels of damage. A simplified expression for displacement-based design was developed and utilized to identify the critical design limit state in a multilevel design.

ACKNOWLEDGMENTS

The research described was supported by the Department of Civil Engineering North Carolina State University. The writer would like to thank the reviewers of the paper for their very careful reading of the manuscript and many useful comments and suggestions.

APPENDIX I REFERENCES

Applied Technology Council (ATC). (1996). ''Improved seismic design criteria for California bridges: Provisional recommendations.'' *Rep. #ATC-32*, Redwood City, Calif.

Calvi, G. M., and Kingsley, G. R. (1995). ''Displacement based seismic design of multi-degree-of-freedom bridge structures.'' *Earthquake Engrg. and Struct. Dyn.*, London, 24(6), 1247–1266.

Commission of the European Communities (EC). (1988). ''Eurocode 8 structures in seismic regions—design part 1, general and building.'' *Rep. EUR 8849 EN*, Brussels, Belgium.

Gulkan, P., and Sozen, M. (1974). ''Inelastic response of reinforced concrete structures to earthquake motions.'' *ACI J.*, 71(12), 604–610.

Jacobsen, L. S. (1930). ''Steady forced vibrations as influenced by damping.'' *ASME Trans.*, 52(1), 169–181.

King, D. J., Priestley, M. J. N., and Park, R. (1986). ''Computer programs for concrete column design.'' *Res. Rep. 86/12*, Dept. of Civil Engineering, University of Canterbury, New Zealand.

Kowalsky, M. J., Priestley, M. J. N., and MacRae, G. A. (1995). ''Displacement-based design of RC bridge columns in seismic regions.'' *Earthquake Engrg. and Struct. Dyn.*, London, 24(12), 1623–1642.

Kowalsky, M. J., Priestley, M. J. N., and Seible, F. (1997). ''Shake table testing of lightweight concrete bridges.'' *Struct. Sys. Res. Proj. SSRP-97/10*, Dept. of Structural Engineering, University of California–San Diego, La Jolla, Calif.

Mander, J. B., Priestley, M. J. N., and Park, R. (1988). ''Theoretical stress-strain model for confined concrete.'' *J. Struct. Div.*, ASCE, 114(8), 1804–1825.

Paulay, T., and Priestley, M. J. N. (1992). *Seismic design of reinforced concrete and masonry buildings*, Wiley, New York.

Priestley, M. J. N. (1993). ''Myths and fallacies in earthquake engineering—conflicts between design and reality.'' *Proc., Tom Paulay Symp.—Recent Devel. in Lateral Force Transfer in Build.*, University of California, San Diego, 229–252.

Priestley, M. J. N., and Kowalsky, M. J. (1998). ''Aspects of drift and ductility capacity of rectangular cantilever structural walls.'' Bulletin of the New Zealand National Society for Earthquake Engineering, *Silverstream*, New Zealand, 31(6), 73–85.

Priestley, M. J. N., Seible, F., and Calvi, G. M. (1996). *Seismic design and retrofit of bridge structures*, Wiley, New York.

Shibata, A., and Sozen, M. (1976). ''Substitute structure method for seismic design in R/C.'' *J. Struct. Div.*, ASCE, 102(1), 1–18.

Takeda, T., Sozen, M., and Nielsen, N. (1970). ''Reinforced concrete response to simulated earthquakes.'' *J. Struct. Div.*, ASCE, 96(12), 2557–2573.

APPENDIX II. NOTATION

The following symbols are used in this paper:

A_g = gross section area;
D = section diameter;
d_{bl} = longitudinal bar diameter;
f'_c = concrete compressive strength;
f_y = longitudinal bar yield stress;
L = cantilever column length;
L_p = plastic hinge length;
M_n = nominal moment capacity;
m_{eff} = effective mass;
P = axial load;
r = second slope stiffness ratio;
T_c = period at maximum spectral displacement;
V_b = base shear;
Δ = displacement;
Δ_c = maximum spectral displacement for 5% damped response curve;
Δ_{tar} = target displacement;
ε_y = longitudinal bar yield strain;
ϕ'_Y = first yield curvature;
ϕ_{DC} = damage control limit state curvature;
ϕ_S = serviceability limit state curvature;
ϕ_Y = yield curvature;
μ_Δ = displacement ductility;
$\mu_{\phi DC}$ = damage control limit state curvature ductility;
$\mu_{\phi S}$ = serviceability limit state curvature ductility;
θ = average elastic rotation; and
ζ_{eff} = equivalent viscous damping.